Multiphase Assembly of Mesoporous−Macroporous Membranes

Dongyuan Zhao,[†,‡] Peidong Yang,[†]
Bradley F. Chmelka,[‡] and Galen D. Stucky*[,†,§]

Chemistry Department, Department of Chemical Engineering, and Department of Materials, University of California, Santa Barbara, California 93106

Received December 16, 1998
Revised Manuscript Received February 22, 1999

The synthesis of inorganic−organic composites and mesoporous materials with structures and functions over different length scales has ramifications in diverse areas, such as large-molecule catalysis, biomolecule separations, miniaturization of electronic devices, chromatographic supports, the formation of semiconductor nanostructures, and the development of medical implants.[1−8] The use of organic structure-directing agents to control the structures of inorganic solids has proven successful for designing patterned materials with dimensions ranging from Angstroms to micrometers.[9−25] Mesoporous (20−300 Å) materials can be obtained by using long-chain surfactant or amphiphilic block copolymers.[10,11,13,15,21,22] Recent reports have demonstrated that stabilized-emulsion[5,14,26] or latex-sphere templating[15−18,24] can be used to create TiO_2, ZrO_2, and SiO_2 structures with pore sizes ranging from 100 nm to 1 μm. Mann and co-workers[20] have coated bacterial threads with silica-surfactant mesophases to combine the macroscopic morphology of the threads with mesoporous length scales. While researchers have concentrated on the organization of patterned inorganic composites with domain separation directed by proteins,[20,27−29] low-molecular-weight surfactants, block copolymer amphiphiles, or preformed polystyrene spheres,[15−18,24] little effort has been devoted to creating phase and domain separation[20,30] by using concentrated solutions of inorganic salts.

A novel procedure has been developed for the synthesis of spongelike silica membranes with three-dimensional (3D) structures that have adjustable mesoscopic and macroscopic porosities. The process utilizes multiphase media comprised of a mesoscopically ordered block copolymer/silica phase that macroscopically separates from an electrolyte phase. This results in hierarchically organized composite structures whose different characteristic length scales can be independently adjusted. Macropore dimensions are established by the sizes of droplets of aqueous electrolytes, such as NaCl, LiCl, KCl, NH_4Cl, or $NiSO_4$. At the interstices separating the electrolyte droplets, amphiphilic block copolymer species assemble in the presence of silica to form well-ordered composite mesophases. Mesoscopic ordering length scales are established by the hydrophobic copolymer blocks, including cosolvent swelling agents. Inorganic−organic composites or porous solids can be formed into contiguous membranes using this approach. Such dual mesoscale/macroscale materials will find utility in processes involving large molecules, where high internal surface areas plus low resistances to mass transport are desirable. Examples of such applications include large-molecule catalysis, biomolecule separations, miniaturization of electronic devices, and chromatographic supports.

The silica membranes were prepared by prehydrolysizing tetraethoxysilane (TEOS) in ethanol solution by an acid-catalyzed process[31,32] to obtain an oligomeric

* To whom correspondence should be addressed.
† Chemistry Department.
‡ Department of Chemical Engineering.
§ Department of Materials.

(1) Stucky, G. D. Presented at the National American Chemical Society Meeting, Orlando, FL, Aug 25−27, 1996.
(2) Lee, T.; Yao, N.; Aksay, I. A. *Langmuir* **1997**, *13*, 3866. Lahiri, J.; Xu, G. F.; Dabbs, D. M.; Yao, N.; Aksay, I. A. *J. Am. Chem. Soc.* **1997**, *119*, 5449. Weiner, S.; Traub, W. *FASEB J.* **1992**, *6*, 879.
(3) Kaji, H.; Nakanishi, K.; Soga, N. *J. Non-Cryst. Solids* **1995**, *185*, 18. Kaji, H.; Nakanishi, K.; Soga, N. *J. Non-Cryst. Solids* **1995**, *181*, 16. Kaji, H.; Nakanishi, K.; Soga, N.; Horii, F. *J. Non-Cryst. Solids* **1992**, *145*, 80.
(4) Aksay, I. A.; Trau, M.; Manne, S.; Honma, I.; Yao, N.; Zhou, L.; Fenter, P.; Eisenberger, P. M.; Gruner, S. M. *Science* **1996**, *273*, 892.
(5) Schächt, S.; Huo, Q.; Voigt-Martin, I. G.; Stucky, G. D.; Schüth, F. *Science* **1996**, *273*, 768.
(6) Roy, D. M.; Linneham, S. K. *Nature* **1974**, *247*, 220.
(7) Yang, P.; Lieber, C. M. *Science* **1996**, *273*, 1836.
(8) Mann, S.; Ozin, G. A. *Nature* **1996**, *382*, 313.
(9) Kresge, C. T.; Leonowicz, M. E.; Roth, W. J.; Vartuli, J. C.; Beck, J. S. *Nature* **1992**, *359*, 710. Beck, J. S.; Vartuli, J. C.; Roth, W. J.; Leonowicz, M. E.; Kresge, C. T.; Schmitt, K. T.; Chu, C. T.-W.; Olson, D. H.; Sheppard, E. W.; McCullen, S. B.; Higgins, J. B.; Schlenker, J. L. *J. Am. Chem. Soc.* **1992**, *114*, 10834.
(10) Zhao, D.; Feng, J.; Huo, Q.; Chmelka, B. F.; Stucky, G. D. *Science* **1998**, *279*, 548.
(11) Zhao, D.; Huo, Q.; Feng, J.; Chmelka, B. F.; Stucky, G. D. *J. Am. Chem. Soc.* **1998**, *120*, 6024.
(12) Huo, Q.; Margolese, D. I.; Ciesla, U.; Feng, P.; Gier, T. E.; Sieger, P.; Leon, R.; Petroff, P. M.; Schüth, F.; Stucky, G. D. *Nature* **1994**, *368*, 317.
(13) Yang, P.; Zhao, D.; Margolese, D. I.; Chmelka, B. F.; Stucky, G. D. *Nature* **1998**, *396*, 152.
(14) Imhof, A.; Pine, D. J. *Nature* **1997**, *389*, 948. Imhof, A.; Pine, D. J. *Adv. Mater.* **1998**, *10*, 697.
(15) Antonietti, M.; Berton, B.; Göltner, C.; Hentze, H. *Adv. Mater.* **1998**, *10*, 154.
(16) Holland, B. T.; Blanford, C. F.; Stein, A. *Science* **1998**, *281*, 538.
(17) Wijnhoven, J. E. G. J.; Vos, W. L. *Science* **1998**, *281*, 802.
(18) Park, S. H.; Qin, D.; Xia, Y. *Adv. Mater.* **1998**, *10*, 1028. Park, S. H.; Xia, Y. *Adv. Mater.* **1998**, *10*, 1045.
(19) Trau, M.; Yao, N.; Kim, E.; Xia, Y.; Whitesides, G. M.; Aksay, I. A. *Nature* **1997**, *390*, 674. Yang, H.; Coombs, N.; Ozin, G. A. *Adv. Mater.* **1997**, *9*, 811.
(20) Davis, S. A.; Burkett, S. L.; Mendelson, N. H.; Mann, S. *Nature* **1997**, *385*, 420.
(21) Tanev, P. T.; Pinnavaia, T. J. *Science* **1995**, *267*, 865; **1996**, *271*, 1267.
(22) Bagshaw, S. A.; Prouzet, E.; Pinnavaia, T. J. *Science* **1995**, *269*, 1242.
(23) Bu, X.; Feng, P.; Stucky, G. D. *Science* **1997**, *278*, 2080.
(24) Yang, P.; Deng, T.; Zhao, D.; Feng, P.; Pine, D. J.; Chmelka, B. F.; Whitesides, G. M.; Stucky, G. D. *Science* **1998**, *282*, 2244.
(25) Huck, W. T. S.; Tien, J.; Whitesides, G. M. *J. Am. Chem. Soc.* **1998**, *120*, 8267.
(26) Sims, S. D.; Walsh, D.; Mann, S. *Adv. Mater.* **1998**, *10*, 151.
(27) Round, F. E.; Crawford, R. M.; Mann, D. G. *'The Diatoms' Biology & Morphology of the Genera;* Cambridge University Press: Cambridge, 1990.
(28) Belcher, A. M.; Wu, X. H.; Christensen, R. J.; Hansma, P. K.; Stucky, G. D. *Nature* **1996**, *381*, 56.
(29) Shen, X. Y.; Belcher, A. M.; Hansma, P. K.; Stucky, G. D.; Morse, D. E. *J. Biol. Chem.* **1997**, *272*, 32472.
(30) Nakanishi, K. *J. Porous Mater.* **1997**, *4*, 67.
(31) Zhao, D.; Yang, P.; Melosh, N.; Feng, J.; Chmelka, B. F.; Stucky, G. D. *Adv. Mater.* **1998**, *10*, 1380. Zhao, D.; Yang, P.; Margolese, D. I.; Chmelka, B. F.; Stucky, G. D. *Chem. Commun.* **1998**, *22*, 2499.

10.1021/cm980782j CCC: $18.00
Published on Web 04/13/1999

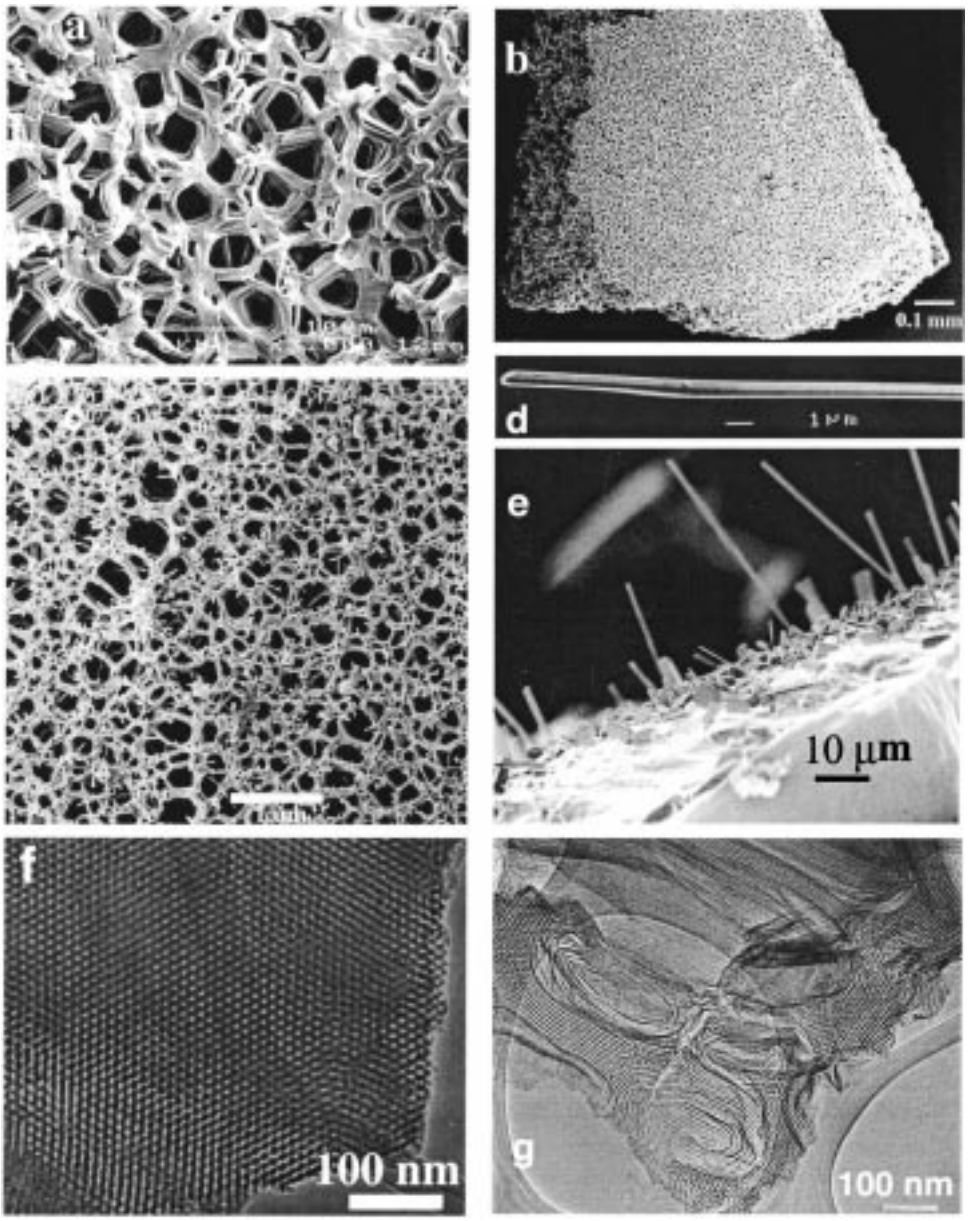

Figure 1. (a, b) Scanning electron micrographs (SEM) at different magnifications of as-synthesized meso−macrostructured silica membranes prepared by using P123 ($EO_{20}PO_{70}EO_{20}$) block copolymer species in NaCl solution after washing with deionized water; (c) an SEM image showing smaller macropores (compared to a), in a silica membrane prepared with a small amount of ethylene glycol under otherwise identical conditions; (d, e) SEM images of (d) an acicular NaCl single-crystal and (e) inorganic salt NaCl crystals co-grown with the silica membrane. The SEM images were obtained on a JEOL 6300-F microscope. Transmission electron micrographs (TEM) of (f) the mesostructured silica struts in the calcined silica membrane of (a) prepared using the block copolymer P123 in NaCl solution and (g), calcined silica membrane of (c) prepared with a small amount of ethylene glycol. The TEM images were acquired on a 2000 JEOL electron microscope operating at 200 kV. For the TEM measurements, the samples were prepared by dispersing the powdered products as a slurry in acetone, after which they were deposited and dried on a holey carbon film on a Cu grid.

silica sol, which was added to a solution of poly(ethylene oxide)-*block*-poly(propylene oxide)-*block*-poly(ethylene oxide) (PEO−PPO−PEO) triblock copolymer and inorganic salts in water and ethanol. The final composition of each mixture was in the range of 1:0.0068∼0.034:0.51∼3.0:18∼65:0.002∼0.04:11∼50/TEOS:copolymer:inorganic salt:H_2O:HCl:EtOH. Porous silica membranes with 3D meso−macrostructures were obtained after drying at room temperature, washing with water to remove residual inorganic salts, and calcining at 500 °C for 6 h in air to remove the block copolymer species.

Figure 1 shows several representative scanning electron microscopy (SEM) and transmission electron microscopy (TEM) images of silica membranes and inorganic salt (NaCl) crystals that are co-grown with the membranes. The silica membranes prepared from NaCl solution show 3D macroscopic network structures and a spongelike morphology (Figure 1a). The reticular 3D network (mean strut thickness ∼ 1 μm) of the silica membrane is made up of continuous interconnected ropelike mesoporous silica which exhibits a high degree

(32) Yang, P.; Zhao, D.; Chmelka, B. F.; Stucky G. D. *Chem. Mater.* **1998**, *10*, 2033.

of mesoscopic ordering (see below). The silica membranes can be as large as $\sim 4 \times 4$ cm^2, depending on the size of the reaction container that is used. The thickness of the silica membranes can be varied from 10 μm to 5 mm.

As shown in Figure 1, parts a and b, the meso−macroporous silica membrane possesses relatively uniform, but poorly ordered, macroscopic organization. The average macropore size of the silica membrane shown here is about $\sim$2 μm ($\pm$0.4) (Figure 1a), but can be selectively varied from $\sim$0.5 μm to $\sim$100 μm by adjusting the rates of macroscopic phase separation and silica gelation. For example, when a small amount of ethylene glycol is added to slow the rate of ethanol evaporation, a small mean macropore size ($\sim$0.5 μm) is obtained, as shown in Figure 1c. Under these conditions, evaporation of the ethanol causes macroscopic phase separation of concentrated aqueous salt solution droplets from the inorganic oxide/block copolymer mesophase. The macropore dimensions are established by the sizes of the salt solution droplets, which are controlled by the rates of EtOH evaporation and silica gelation, and around which mesoscopically ordered silica−block copolymer walls are formed. These silica/block copolymer walls have a strut-like appearance and a wall thickness of several hundred nanometers that diminishes with the size of the macropore. When the EtOH evaporation rate is high, large droplets form, which cannot coalesce because of high gel viscosity. Under these conditions, the mean macropore size of the silica membranes can be as large as $\sim$10 μm, with the strut thicknesses increasing correspondingly. In addition, the macroscopic structure of the silica membranes is changed to a 2D open-pore channel structure.

The morphologies of the inorganic salt crystals are also affected by the nature of the block copolymer surfactant species. For example, without the amphiphilic block copolymer, cubic crystals of NaCl as large as $\sim$100 μm can be grown in the solution of water and ethanol. However, in the presence of the block copolymer Pluronic P123 ($EO_{20}PO_{70}EO_{20}$) under our synthesis conditions, NaCl crystals show an acicular needlelike ($\sim$1 μm in diameter) morphology (Figure 1d,e), with lengths up to $\sim$1 cm. When more hydrophilic block copolymers such as Pluronic F127 ($EO_{106}PO_{70}EO_{106}$) are used, the mesoporous silica is assembled around cubic-shaped NaCl crystals (Figure 2a), which in this case serve to organize macroscopically the growth and form of the mesoporous silica. The morphology of the silica membrane can be modified by changing the concentration of the inorganic salt. Whereas low concentrations result in an inhomogeneous silica membrane, a grapevine strut morphology with a high degree of mesoporosity makes up the silica membrane obtained at higher salt concentrations, as shown in Figure 2b.

Besides NaCl, other inorganic salts such as LiCl, KCl, NH_4Cl, $NiSO_4$, or $NaClO_3$[33] can be used to form the silica membranes. For example, when $NiSO_4$ is used under the above conditions, a disklike morphology of $NiSO_4$ crystal is observed (Figure 2c) at the bottom of the silica membranes (Figure 2d), confirming that

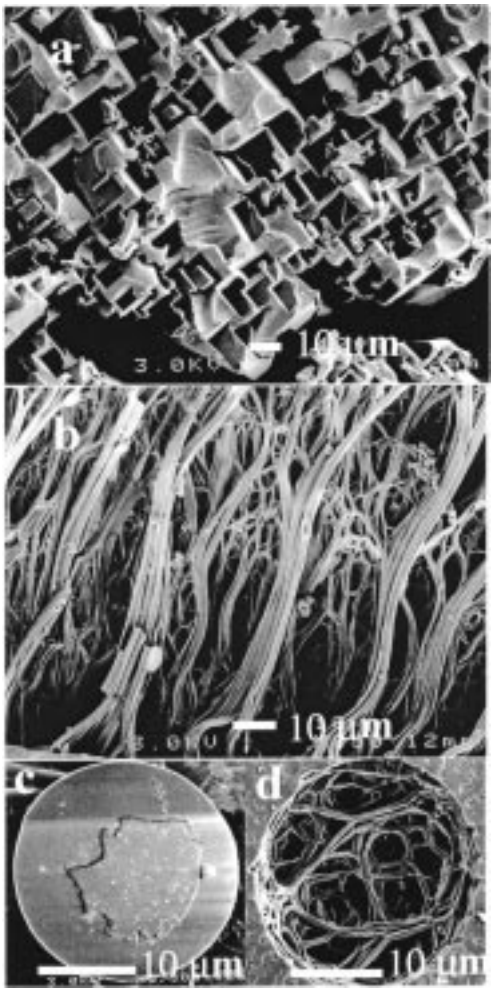

Figure 2. SEM images of (a) a silica membrane prepared using a F127 block copolymer ($EO_{106}PO_{70}EO_{106}$) in NaCl solution; (b) a silica membrane with grapevine morphology prepared with a high concentration of NaCl; (c) disklike $NiSO_4$ inorganic salt crystals grown on the bottom of the silica membranes, (d) an as-synthesized silica membrane prepared by using the P123 block copolymer in $NiSO_4$ solution, which shows the top of the membrane containing a disk window the same size as that of the $NiSO_4$ crystal and the inside of a spongelike silica structure.

crystallization of the inorganic salts is influenced by block copolymers. The morphology of the silica membranes depends on the electrolyte strengths of these salts. For example, when LiCl, KCl, or NH_4Cl are used (which are comparable to NaCl), similar spongelike membrane morphologies are observed, although the strut networks of the various silica membranes are somewhat different. However, when salts with higher electrolyte strengths, such as Na_2SO_4 or $MgSO_4$, are used, the macroscopic structures consist of silica networks made up of grapevine, toroid, pinwheel, dish, or gyroid morphologies.

The mesoscopic ordering in these silica membranes, which are formed by the cooperative assembly of inorganic silica/amphiphilic block copolymer species is controlled by aggregation and microphase separation behaviors of the block copolymer. Such ordering can be characterized by low-angle X-ray diffraction patterns (Figure 3) and transmission electron microscopy (TEM) (Figure 1f,g). The silica membranes synthesized using

(33) Kondepudi, D. P.; Kaufman, R. J.; Singh, N. *Science* **1990**, *250*, 975. McBride, J. M.; Carter, R. L. *Angew. Chem., Int. Ed. Engl.* **1991**, *30*, 293.

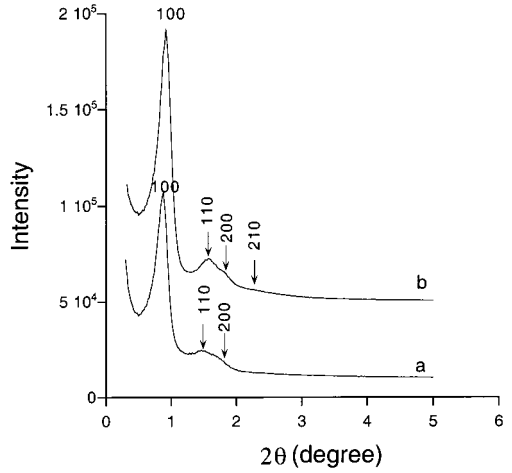

Figure 3. Powder X-ray diffraction (XRD) patterns of (a) as-synthesized and (b) calcined meso−macro silica membranes prepared using the amphiphilic polyalkylene oxides P123, $EO_{20}PO_{70}EO_{20}$ block copolymer. The chemical composition of the reaction mixture was 1:0.017:0.01:4 × 10^{-5}:0.72:0.33/g of copolymer:mol of NaCl:mol of TEOS:mol of HCl:mol of H_2O:mol of EtOH. The XRD patterns were acquired on a Scintag PADX diffractometer using Cu K_α radiation.

P123 triblock copolymer, and after removal of NaCl by washing, show a typical hexagonal (*p*6*mm*) XRD pattern for mesoporous materials with four diffraction peaks (a = 118 Å) (Figure 3a).[10,11] After calcination at 500 °C in air for 6 h, the four-peak XRD pattern is preserved and the intensities of the diffraction peaks are increased (Figure 3b), indicating that the *p*6*mm* mesoscopic ordering (a = 111 Å) is retained and thermally stable. The cell parameters of the mesoscopically ordered silica membranes can be varied by using different triblock copolymers, for example, a = 101 Å for Pluronic P103 ($EO_{17}PO_{85}EO_{17}$) and a = 73.5 Å for Pluronic P65 ($EO_{26}PO_{39}EO_{26}$). These materials both have well-ordered 2D hexagonal (*p*6*mm*) mesoscopic structures.

TEM images (Figure 1f) of calcined silica membranes prepared using P123 block copolymer species in NaCl solution further confirm that the silica struts of the membranes are highly ordered 2D *p*6*mm* hexagonal mesostructures, which form extended one-dimensional (1D) channels. The TEM image in Figure 1g from a silica membrane with small macropores (∼0.5 μm from SEM, Figure 1c, prepared with a small amount of ethylene glycol) shows that the ropelike struts of the silica membranes are made up of looplike mesoscopic silica with oriented 1D channel arrays parallel to the long axes. These ropelike silicas form a three-dimensional (3D) silica network with a macroporous structure. When the higher molecular weight F127 block copolymer species are used as the mesoscopic structure-directing agents, a silica membrane with a cubic mesostructure (*Im*3*m*) is obtained, on the basis of XRD and TEM results. This provides the accessibility of the meso−macropore systems to diffusing guest species.

SEM images of the silica membranes obtained after calcination of the materials in air at 500 °C show that the spongelike macrostructure is retained. Thermal gravimetric and differential thermal analyses (TGA and DTA) show that the block copolymer species of the silica membrane can be removed at temperatures as low as 190 °C, indicating that the interactions between silica

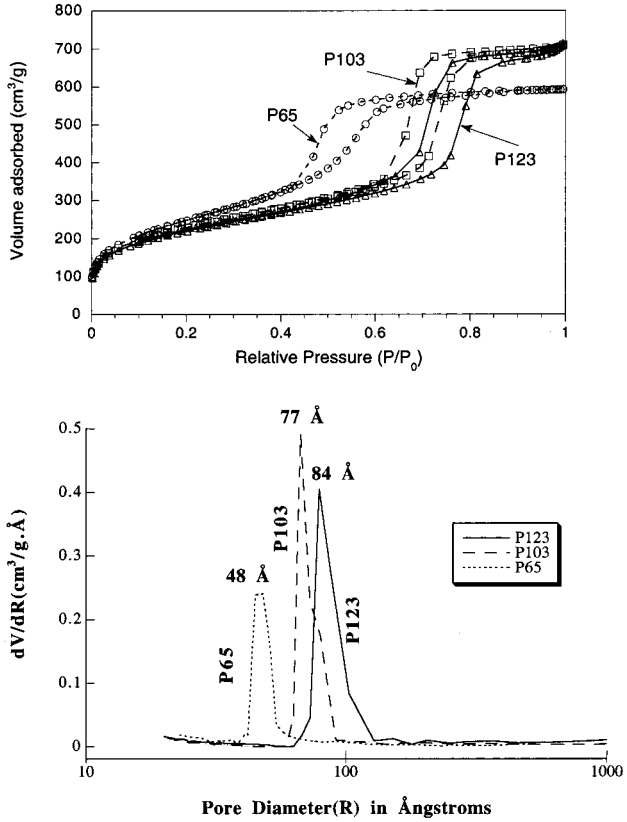

Figure 4. Nitrogen adsorption−desorption isotherm plots (top) and pore size distribution curves (bottom) for calcined meso−macro porous silica membranes prepared in a NaCl solution using different block copolymers: P65 ($EO_{26}PO_{39}EO_{26}$), P103 ($EO_{17}PO_{85}EO_{17}$), and P123 ($EO_{20}PO_{70}EO_{20}$). The isotherms were measured using a Micromeritics ASAP 2000 system. Data were analyzed by using the BdB (Broekhoff and de Boer) model.[34] The differential pore size distribution curves were obtained from an analysis of the adsorption branch of the isotherm. The BET sample was pretreated at 200 °C overnight on the vacuum line.

species and block copolymer species are relatively weak. The weak interactions also result in the removal of 84 wt % of the block copolymer in the silica membranes after washing with water. Even without calcination, these washed silica membranes already show nitrogen sorption behavior similar to that observed for calcined silica membranes, indicating that both the macroporous (∼2 μm) and mesoporous (60 Å) channels are readily accessible.

Representative nitrogen adsorption/desorption isotherms and the corresponding pore size distributions (analyzed by using the Broekhoff and de Boer model[34]) are shown in Figure 4. The spongelike silica membranes prepared using P123 block copolymers in a NaCl solution yield an isotherm (type IV) with H_1-type hysteresis that is typical of mesoporous materials with 1D cylindrical channels. A narrow pore size distribution with a mean value of 84 Å is also obtained for both the adsorption and desorption processes. This material has a Brunauer−Emmett−Teller (BET) surface area of 660 m^2/g and a pore volume of 1.1 cm^3/g. The mesoscopic pore size of the silica membranes prepared in NaCl solution depends on the amphiphilic block copolymer

(34) Broekhoff, J. C. P.; deBoer, J. H. *J. Catal.* **1967**, *9*, 8. *J. Catal.* **1968**, *10*, 153. *J. Catal.* **1968**, *10*, 368.

species used. For example, the materials prepared with lower molecular weight P103 and P65 block copolymers show similar isotherms and exhibit pore sizes of 77 and 48 Å, BET surface areas of 720 and 930 m^2/g, and pore volumes of 1.12 and 0.99 cm^3/g, respectively (Figure 4). When higher molecular weight F127 block copolymer species are used, a silica membrane with a cubic ($Im3m$) mesoscopic structure is obtained, which shows an isotherm with H_2-type hysteresis, a narrow pore size distribution with a mean value of 105 Å, a BET surface area of 1003 m^2/g, and a pore volume of 0.8 cm^3/g.

On the basis of compositional and structural change as a function of reaction time studied by elemental analysis, SEM, and XRD, we postulate that the macroscopic silica structure is formed through a multiphase process. This involves aqueous inorganic salt solution droplets, which macroscopically phase-separate from the assembling inorganic oxide−block copolymer mesophase during evaporation of the ethanol cosolvent. The triblock copolymer directs mesoscale organization, forming hydrophilic/hydrophobic aggregates; the hydrophilic EO_x moieties of the triblock copolymer interact with the hydrolyzed and polymerizing silica species to direct the formation of a highly ordered mesoscale structure that is built into the struts of the macroscale membrane shown in Figure 1a. Surface energies and forces at the strong electrolyte−triblock copolymer/silica interface determine the nonequilibrium development of the mesoscopic and macroscopic structures observed. With the evaporation of ethanol and water during the process, the inorganic salt solution becomes more concentrated and two domains are evident, one water-rich, where most of the inorganic salt is concentrated, and another water-poor, corresponding to the assembled silica and block copolymer species. The separate phases, however, remain in contact, such that the silica−block copolymer mesophase permeates the interstitial regions between the small salt solution droplets.[25] During this process, crystallization of the electrolyte can take place in unexpected ways, for example, resulting in the needle-like NaCl crystals within the macropores (Figure 1d, e). Alteratively, if a more hydrophilic triblock copolymer is used, cubic NaCl crystals can form and become coated with a silica/block copolymer mesophase composite (Figure 2a).

In summary, spongelike silica membranes with 3D meso−macrostructures have been synthesized by a novel multiphase process of acid-catalyzed silica sol−gel chemistry[12,31,32] in the presence of inorganic salts and self-assembling block copolymers. Inorganic salts play an important role in the formation of the meso−macro silica structures that are grown at the interface of inorganic salt solution droplets. The silica membranes with 3D meso−macrostructured silica network can be varied, depending on the electrolyte strength of the inorganic salts and the amphiphilic block copolymer structure-directing agents. The macropore dimensions can be controlled according to the sizes of the salt solution droplets, which can be adjusted by regulating the evaporation rate of the solvent. The mesoscopic structures can be highly ordered 2D honeycomb or 3D cubic configurations, as established by the assembly properties of the amphiphilic block copolymer species. The silica membranes are thermally stable and exhibit large surface areas and pore volumes. The results are of general importance for understanding multiphase processes in strong electrolyte media, including the formation of diatoms and biosilica structures in salt-water environments.

Acknowledgment. This work was supported by the National Science Foundation under Grants DMR 95-20971 (G.D.S.) and CTS-9871970 (B.F.C.) and the U.S. Army Research Office under Grant DAAH04-96-1-0443. This work made use of MRL Central Facilities supported by the National Science Foundation under Award No. DMR-9632716. B.F.C. is a Camille and Henry Dreyfus Teacher-Scholar and an Alfred P. Sloan Research Fellow. We thank BASF (Mt. Olive, NJ) for providing the block copolymer surfactants.

CM980782J